


RESEARCH

Open Access



Ultrasound-guided renal subcapsular transplantation of mesenchymal stem cells for treatment of acute kidney injury in a minipig model: safety and efficacy evaluation

Tuo Xiao^{1,2†}, Yuhao Chen^{1†}, Bo Jiang^{3†}, Mengjie Huang¹, Yanjun Liang¹, Yue Xu¹, Xumin Zheng¹, Wenjuan Wang¹, Xiangmei Chen^{1*} and Guangyan Cai^{1*} 

Abstract

Background Acute kidney injury (AKI) is a major global public health concern with limited treatment options. While preclinical studies have suggested the potential of mesenchymal stem cells (MSCs) to repair and protect injured kidneys in AKI, clinical trials using transarterial MSCs transplantation have yielded disappointing results. This study aimed to investigate the feasibility and safety of minimally invasive renal subcapsular transplantation of MSCs for treating AKI in a minipig model, ultimately aiming to facilitate the clinical translation of this approach.

Methods A novel AKI minipig model was established by combining cisplatin with hydration to evaluate the effectiveness of potential therapies. Renal subcapsular catheterization was successfully achieved under ultrasound guidance. Subsequently, the efficacy of renal subcapsular MSCs transplantation was assessed, and the biological role of the tryptophan metabolite kynurenine (Kyn) in AKI was elucidated through both in vivo and in vitro experiments.

Results The method of pre-hydration at 4% of body weight, followed by post-cisplatin (3.8 mg/kg) hydration at 2% of body weight, successfully established a cisplatin-induced AKI minipig model with a survival time exceeding 28 days, closely mimicking the clinical characteristics of typical AKI patients. Additionally, we discovered that multiple MSCs transplantations promoted renal function recovery more effectively than single transplantation via the renal subcapsular catheter. Furthermore, elevated levels of Kyn were observed in kidney during AKI, which activated the aryl hydrocarbon receptor (AhR)-mediated NF- κ B/NLRP3/IL-1 β signaling pathway in tubular epithelial cells, thereby exacerbating inflammatory injury.

Conclusions Ultrasound-guided renal subcapsular transplantation of mesenchymal stem cells is a safe and effective therapeutic approach for AKI, with the potential to bring about significant clinical advancements in the future.

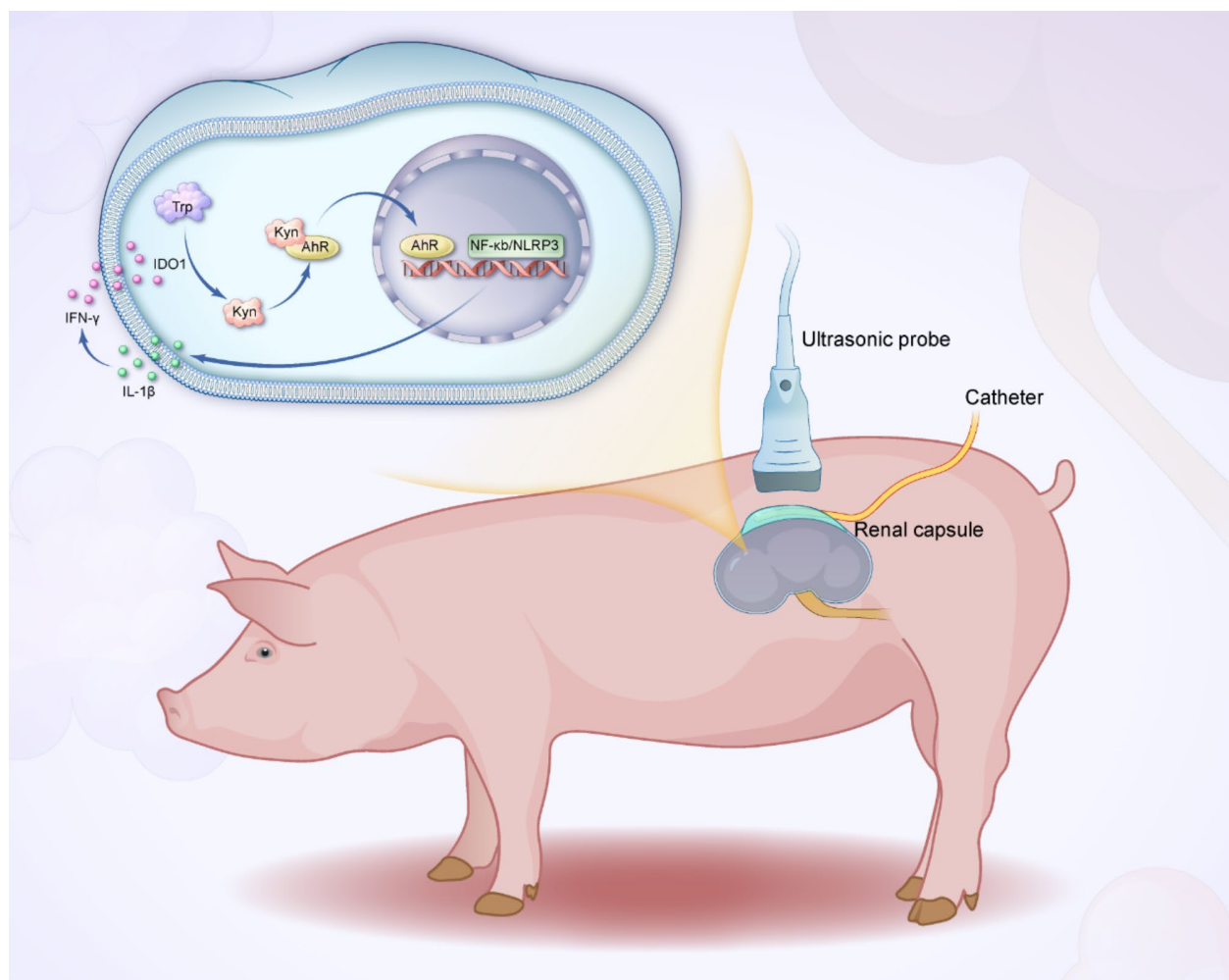
[†]Tuo Xiao, Yuhao Chen, and Bo Jiang contributed equally to this work.

*Correspondence:
Xiangmei Chen
xmchen301@126.com
Guangyan Cai
caiguangyan@sina.com

Full list of author information is available at the end of the article



© The Author(s) 2025. **Open Access** This article is licensed under a Creative Commons Attribution-NonCommercial-NoDerivatives 4.0 International License, which permits any non-commercial use, sharing, distribution and reproduction in any medium or format, as long as you give appropriate credit to the original author(s) and the source, provide a link to the Creative Commons licence, and indicate if you modified the licensed material. You do not have permission under this licence to share adapted material derived from this article or parts of it. The images or other third party material in this article are included in the article's Creative Commons licence, unless indicated otherwise in a credit line to the material. If material is not included in the article's Creative Commons licence and your intended use is not permitted by statutory regulation or exceeds the permitted use, you will need to obtain permission directly from the copyright holder. To view a copy of this licence, visit <http://creativecommons.org/licenses/by-nc-nd/4.0/>.

Graphical abstract

Keywords Acute kidney injury, Cisplatin, Renal subcapsular transplantation, Ultrasound, Mesenchymal stem cells

Introduction

Acute kidney injury (AKI) is a syndrome characterized by a rapid decline in kidney function within hours or days. It affects people of all ages, both in the community and in hospitals, and is a significant cause of death [1]. Approximately 20% of hospitalized patients develop AKI, with half requiring renal replacement therapy [2, 3], and the in-hospital mortality rate exceeds 50% for severe cases [4, 5]. The incidence of AKI has been rising in recent years due to factors such as an aging population, increased comorbidity rates, the use of nephrotoxic drugs, and more invasive surgeries. It is estimated that AKI causes 2 million deaths worldwide each year, posing a serious threat to human health and a significant challenge to global healthcare systems [6, 7]. As outlined in the KDIGO AKI clinical practice management guidelines and expert consensus [8–10], current approaches

to managing AKI predominantly emphasize supportive care, highlighting the imperative need for investigation of new treatment strategies to effectively address clinical demands.

Mesenchymal stem cells (MSCs), a type of adult stem cell characterized by their self-renewal and differentiation potential, exhibit multiple differentiation lineages, high proliferation ability, immunomodulatory properties, and self-replication ability, making them promising candidates for novel AKI therapies [11]. Preclinical studies have demonstrated the efficacy of MSCs in alleviating AKI models induced by ischemia-reperfusion, nephrotoxic drugs, sepsis, and cecal ligation and puncture [12, 13]. However, clinical trials have yielded disappointing results, potentially due to low renal implantation and retention rates, as well as the risk of aggravating renal blood flow problems associated with intravascular

transplantation [14–16]. Our previous research has shown promising therapeutic effects using renal subcapsular transplantation of MSCs [17, 18]. The renal capsule offers advantages, including abundant blood vessels and an immune-privileged environment, which protects the graft from the innate immune system [19] and avoids thrombosis risks associated with high cell doses. However, current surgical techniques for subcapsular transplantation are invasive and require bioadhesives to fix the transplanted cells and prevent them from overflowing the capsule [17, 18], hindering its clinical translation.

The kynurenine pathway (KP), recognized as the primary metabolic route for tryptophan (Trp) degradation [20] and a significant contributor to energy metabolism and inflammation [21], produces its metabolite, kynurenine (Kyn), which activates the aryl hydrocarbon receptor (AhR), thereby inducing oxidative stress, inflammatory responses, and immune reactions, while potentially facilitating disease progression [22–24]. Although animal models and patients with AKI exhibit significantly elevated Kyn levels [25–27], its precise biological role in AKI remains unclear.

In this study, the ultrasound-guided and minimally invasive renal subcapsular transplantation of MSCs for the treatment of AKI in minipigs was investigated, with the objective of addressing the challenges encountered in the clinical application of MSCs. Additionally, the study investigated the biological effects of the tryptophan metabolite Kyn in AKI, providing further insights into the pathogenesis of AKI.

Methods

AKI model and experimental design

This study involved 29 male Bama minipigs (15–20 kg) obtained from Beijing Shichuang Century Minipig Breeding Base. The animals were housed at the Animal Experimental Center of the Chinese People's Liberation Army General Hospital with ad libitum access to water and standard feed provided twice daily.

Cisplatin injection (Nuoxin, Haosen) was prepared at a concentration of 0.1 mg/ml, and AKI was induced by intravenous injection of 3.8 mg/kg cisplatin [28] combined with various hydration regimens. Four minipigs were randomly subjected to the following interventions: (1) Cisplatin administration without subsequent hydration; (2) Cisplatin administration followed by a 2% body weight hydration fluid infusion; (3) Cisplatin administration followed by a 4% body weight hydration fluid infusion; (4) A 4% body weight hydration fluid infusion administered one day prior to cisplatin, followed by a 2% body weight hydration fluid infusion after cisplatin administration. Subsequently, six minipigs were randomly divided into control and cisplatin groups to verify the stability of the model established by Method 4.

P6–P8 generations of MSCs were used to treat AKI minipigs [17]. Sixteen minipigs were randomly divided into the following four groups: sham group, exposed to hydration and without cisplatin and MSCs transplantation; cisplatin group, exposed to hydration and cisplatin and without MSCs transplantation; single transplantation group, exposed to hydration and cisplatin and injected MSCs (2×10^6 cells/kg) through the catheter at 6 hours after cisplatin injection; multiple transplantation group, exposed to hydration and cisplatin and injected MSCs (2×10^6 cells/kg, 1×10^6 cells/kg and 1×10^6 cells/kg) through the catheter at 6 hours, 2 days and 4 days after cisplatin injection respectively, and were euthanized on the 7th day (Fig. 4A). All minipigs underwent catheterization beneath the left renal capsule, and 5 ml of saline solution or saline solution containing MSCs was injected through the catheter.

Blood and kidney tissue samples

Blood samples were collected from veins of lower limbs, and serum creatinine (SCr) and blood urea nitrogen (BUN) were detected by Roche cobas 8000 automatic biochemical immune analysis system of Biochemistry Department of PLA General Hospital. Kidney tissue samples were collected from miniature pigs by ultrasound-guided percutaneous renal puncture after anesthesia with Xylazine hydrochloride (Huamu) and Zoletil 50 (Virbac) or execution by intravenous injection of 10% potassium chloride after anesthesia, fixed with 4% paraformaldehyde, and embedded in paraffin after dehydration.

Histologic analysis

Issue staining procedures, including PAS, Masson, and Sirius scarlet staining, were performed as previously described [17]. For immunohistochemistry, sections were incubated with 3% hydrogen peroxide, followed by citrate antigen retrieval and blocking with goat serum (G1208, Servicebio). Primary antibodies (KIM-1, Bioss; Vimentin, Proteintech; AhR, GeneTex) were incubated overnight at 4 °C. Species-specific secondary antibodies were then applied, followed by hematoxylin staining for nuclei visualization. Terminal deoxynucleotidyl transferase dUTP nick end labeling (TUNEL) staining was performed on minipig kidney tissue sections using a kit from Beyotime according to the manufacturer's instructions. Images were captured at 200x magnification using an Olympus FV10-ASW microscope for PAS, Masson, Sirius scarlet, and immunohistochemistry staining. TUNEL staining was imaged using a Laser Scanning Confocal Microscope Olympus FV3000.

Renal tubular injury was evaluated using PAS staining. The percentage of tubules exhibiting cell necrosis, brush border loss, abnormal formation, dilation, and inflammatory cell infiltration was assessed according

to a previously described scoring system [28]. Scores were assigned as follows: no injury, 0; $\leq 10\%$, 1; 11–20%, 2; 21–30%, 3; 31–40%, 4; $>41\%$, 5. At least 4–6 random fields of view were evaluated per sample, and the average score was used as the final score for each animal. Masson staining was quantified using ImageJ software (National Institutes of Health, Bethesda, MD).

Renal subcapsular catheterization

Following anesthesia, the minipigs underwent routine skin disinfection. Using ultrasound guidance (M9, Mindray), the inferior pole of the left kidney was identified, and a suitable puncture site was selected. A small incision (3 mm) was made at the puncture site with a scalpel blade. Saline solution was then injected through a disposable needle (0.7 × 80 mm, KDL) under ultrasound guidance to create a space between the kidney tissue and the capsule. Subsequently, a central venous catheter set (ES-04301, ARROW) was inserted through the puncture site, and the safety of catheter placement was confirmed in three minipigs. Detailed procedural steps can be found in the Supplement Methods and Materials.

Cell experiments

Kidneys were harvested from C57BL/6 mice aged 4 to 6 weeks (Sbeifu Biotechnology Co., Ltd.) with pentobarbital anesthesia (euthanized via decapitation) to isolate primary renal tubular epithelial cells (RTECs) as previously described [29]. The isolated cells were cultured in RPMI-1640 medium (Gibco) supplemented with 1x ITS-G (Thermo Fisher), 20 ng/ml EGF (Thermo Fisher), 10% FBS (Gibco), and 1% penicillin-streptomycin (Gibco) at 37 °C and 5% CO₂ in a cell culture incubator.

Shanghai Hengyuan Biotechnology Co., Ltd. designed and produced siRNA targeting the mouse AhR gene, with the siRNA sequence including a sense strand: 5'-CCUC CACUAUCCAAGAUUATT-3' and an antisense strand: 5'-UAAUUGGAUAGUGGAGGTT-3'. Once the cells reached 30–50% confluence, transfection with the siRNA was performed using Lipofectamine 2000 (Thermo Fisher) for 6 h.

The primary RETCs were treated with IL-1 β (C402, Novoprotein), IFN- γ (C746, Novoprotein), or both for 24 h and then processed for ELISA (EM1862, Finetest) and western blotting analysis, respectively. The normal or siRNA-transfected primary RETCs were treated with Kyn (HY-104026, MCE) for 24 h to assess the biological effects of Kyn. All cell experiments were repeated three times for reproducibility.

Immunoblotting analysis

Kidney tissue and cells were homogenized in RIPA (89900, Thermo Fisher) with PMSF (P0100, Solarbio), and the cells and tissue lysate were centrifuged at 12,000 rpm

and 4 °C for 30 min to remove tissue or cell fragments. Immunoblotting was performed to detect the target protein using the designated antibodies. The intensity of the immunoblot bands was quantified using ImageJ software. Primary and secondary antibodies used are listed in supplementary Table S1.

Statistical methods

All results were presented as mean \pm standard deviation. Statistical analyses were performed using GraphPad Prism 8 software. Statistical comparisons were made using an unpaired t-test between two groups and a one-way analysis of variance (ANOVA) followed by Tukey's multiple comparison test between multiple groups. Repeated measures data were analyzed using a two-way ANOVA test. A p-value of less than 0.05 was considered statistically significant.

Results

AKI minipig model induced by cisplatin combined with hydration

Leveraging our prior experience establishing an AKI minipig model with cisplatin (3.8 mg/kg) [28], we employed hydration to mitigate the nephrotoxicity of high-dose cisplatin [30], aiming to extend the survival time of experimental animals. Figure 1A and B depict the outcomes of four hydration methods used to establish the model. Method 1 (no hydration) resulted in a 10-day survival time. Method 2 (2% body weight hydration after cisplatin infusion) increased survival time to 17 days. Method 3 (4% body weight hydration after cisplatin) only caused slight increases in serum creatinine (SCr) and blood urea nitrogen (BUN), falling short of the diagnostic criteria for AKI. However, Method 4 (4% body weight pre-hydration followed by 2% body weight hydration after cisplatin) led to significant increases in serum SCr and BUN, with a survival time exceeding 28 days, closely mimicking the clinical characteristics of typical AKI patients [31]. The stability of the model established using Method 4 required further validation.

Stability of cisplatin combined with hydration to construct AKI minipig model

To validate the stability of the cisplatin-hydration model, we repeated the experiment using Method 4 to dynamically assess pathological changes in renal tissues, SCr, and BUN throughout the course of AKI onset and recovery (Fig. 2A and B) and the consistent results strongly support the stability of the model. Furthermore, we evaluated renal tubular injury and apoptosis indicators on day 3 (Fig. 2E), while the assessments on day 28 focused on renal tissue fibrosis and cell proliferation indicators (Fig. 2F).

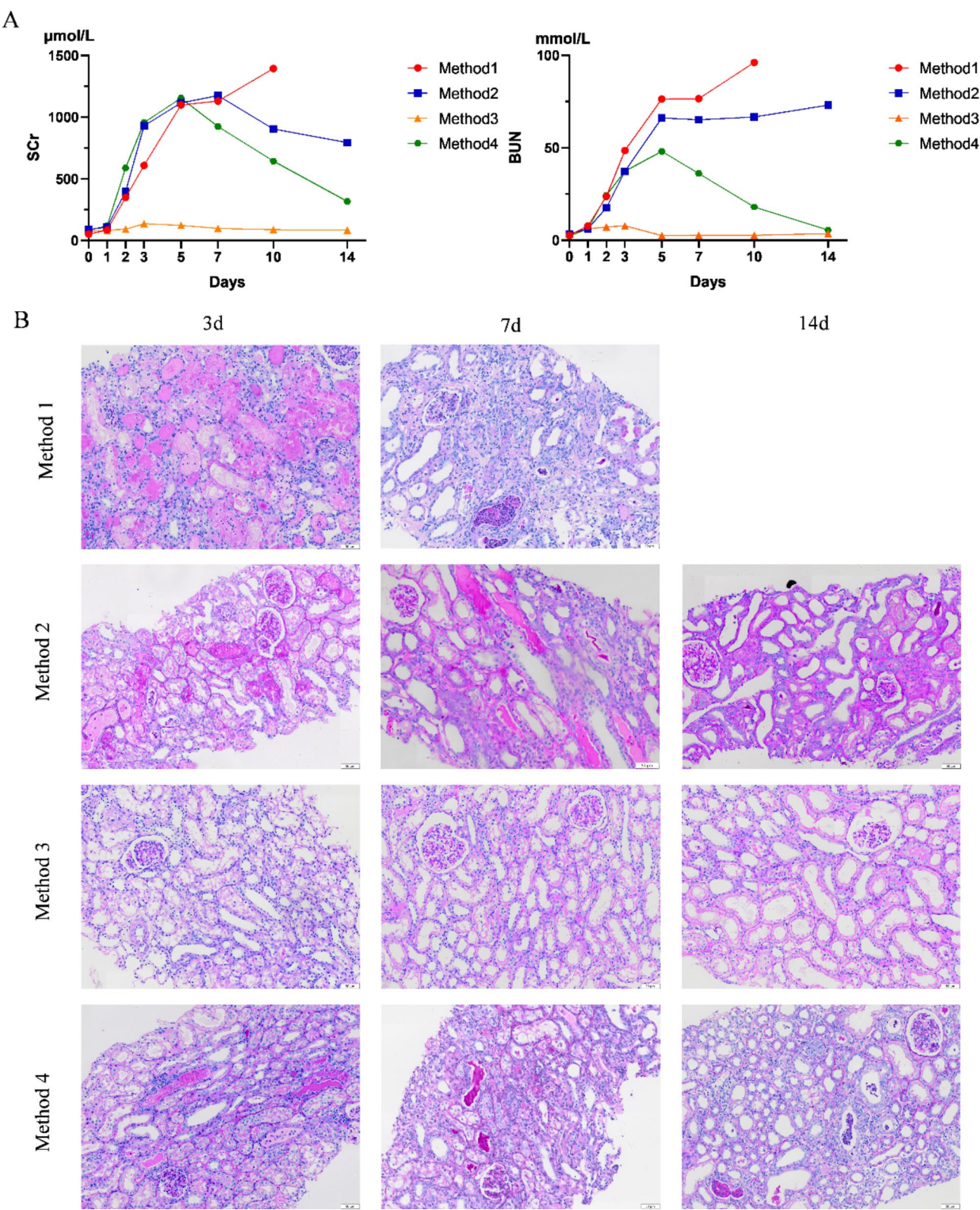


Fig. 1 AKI minipig model induced by cisplatin combined with hydration **(A)** Serum Scr and BUN of models induced by cisplatin with multiple hydration patterns ($n=1$). **(B)** Periodic acid-Schiff (PAS) staining of models induced by cisplatin with multiple hydration patterns ($n=1$)

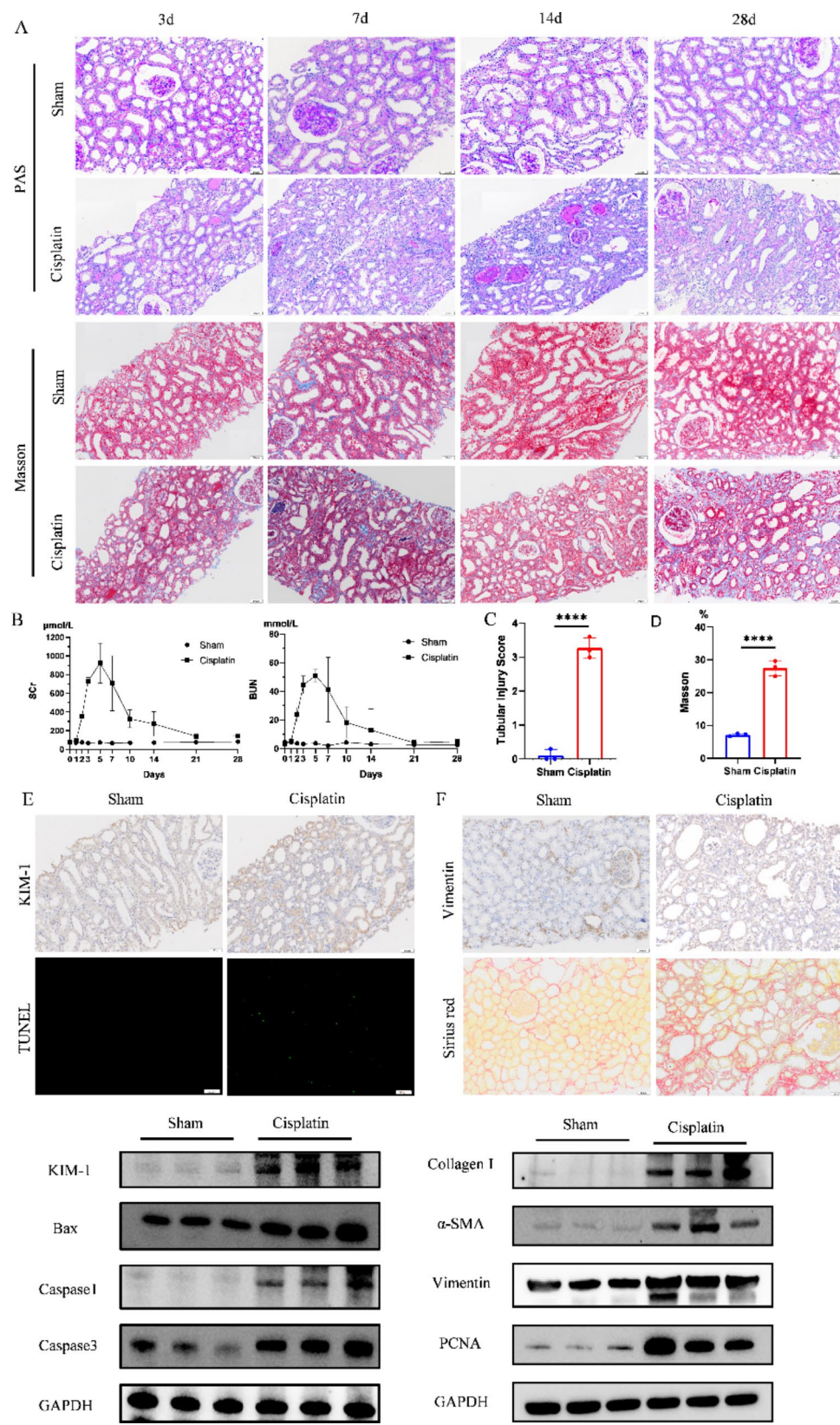


Fig. 2 (See legend on next page.)

(See figure on previous page.)

Fig. 2 Stability of cisplatin combined with hydration to construct AKI minipig model **(A)** PAS and Masson staining of sham and cisplatin group ($n=3$). **(B)** Serum Scr and BUN of sham and cisplatin group ($n=3$). **(C)** Semi-quantitative analysis of PAS staining at 3d ($n=3$). **(D)** Semi-quantitative analysis of Masson staining at 28d ($n=3$). **(E)** KIM-1 on immunohistochemistry (IHC), TUNEL and KIM-1, Bax, Caspase1, and Caspase3 on immunoblotting at 3d ($n=3$). **(F)** Vimentin on IHC, Sirius red staining and Collagen I, α -SMA, Vimentin, and PCNA on immunoblotting at 28d ($n=3$). **(G)** IDO1, KMO, KYNU, HAAO, and QRPT on immunoblotting at 3d and 28d ($n=3$). ****, $p < 0.001$. Full-length blots are presented in Supplementary Immunoblotting Figs. 1–18

To investigate changes in the renal kynurenine pathway during cisplatin-induced AKI, we examined protein expression levels of key enzymes on day 3 and day 28: indoleamine 2,3-dioxygenase 1 (IDO1), kynurenine 3-monooxygenase (KMO), kynureninase (KYNU), hydroxyanthranilic acid 3,4-dioxygenase (HAAO), and quinolinate phosphoribosyltransferase (QRPT) (Fig. 2G). Compared to the sham group, the cisplatin group displayed increased expression of upstream enzymes (IDO1, KMO, KYNU, HAAO) in the kynurenine pathway [32–34], suggesting enhanced metabolite production; conversely, the expression of downstream enzyme (QRPT) was decreased [35], indicating a potential accumulation of intermediate metabolites within the pathway.

Ultrasound-guided renal subcapsular catheterization and safety evaluation

Under ultrasound guidance, renal capsule was separated from renal parenchyma using fluid isolation [36] (Fig. 3A). A guidewire was then inserted through the guide needle (Fig. 3B and C), followed by catheter placement along the guidewire (Fig. 3D). Contrast-enhanced ultrasound was used to visualize the distribution of liquid within the renal capsule after catheter injection. When the injection volume increased, the contrast agent began to flow out of the renal capsule along the catheter channel (Fig. 3F) after initially dispersing uniformly along the catheter and remaining contained within the capsule (Fig. 3E and F). This discovery implies that modest amounts of liquid are kept by the renal capsule, indicating a restricted capacity for liquid retention.

Fluid accumulation within the renal capsule can potentially compress the renal parenchyma, leading to increased renal resistance index (RRI) and hypertension [37, 38]. To assess the safety of subcapsular catheterization, we monitored vital signs and RRI at five time points: before catheterization, after catheterization, and following cumulative fluid injections of 100 ml, 150 ml, and 200 ml (Fig. 3G). Our findings demonstrated no statistically significant changes in heart rate (HR), systolic blood pressure (SBP), diastolic blood pressure (DBP), oxygen saturation (SpO_2), or RRI across the five time points (Fig. 3I). Notably, diastolic blood pressure exhibited a downward trend, which could be attributed to the decrease in myocardial contractility and systemic vascular resistance associated with prolonged sevoflurane anesthesia [39]. These results collectively suggest that short-term isolated fluid accumulation during

subcapsular catheterization does not significantly compress the kidneys.

Multiple renal subcapsular transplantation of MSCs promoting renal recovery

Both the cisplatin and single-transplantation groups had substantially higher blood Scr and BUN levels than the sham group (Fig. 4A). In contrast, the multiple-transplantation group exhibited a progressive decrease in Scr and BUN levels starting at day 3, reaching levels close to the sham group by day 7. These findings suggest improved renal function following multiple MSCs transplantations. Furthermore, the number of TUNEL-positive cells, a marker of cell death, was significantly lower in the multiple-transplantation group compared to the cisplatin and single-transplantation groups (Fig. 4B). Additionally, protein expression levels of KIM-1 (a marker of renal injury), Bax, Caspase-1, and Caspase-3 (apoptotic markers) were significantly downregulated in the multiple-transplantation group compared to the other two groups (Fig. 4C). These results collectively indicate that multiple renal subcapsular transplantation of MSCs could promote renal functional recovery and alleviate cisplatin-induced renal injury more effectively than single transplantation or treatment with cisplatin alone.

MSCs alleviating renal tryptophan metabolism disorder and kyn-mediated AhR/NF- κ B/NLRP3 pathway

Renal tissue metabolomic analysis revealed significant increases in Kyn, Kynurenic acid (KYNA), xanthurenic acid (XA), and Quinolinic acid (QA), intermediate metabolites of the tryptophan kynurenine pathway, in the cisplatin group compared to the sham group [27]. KYNA and QA were downregulated, and Kyn and XA exhibited a downward tendency in the multiple MSCs transplantation group (Fig. 5A). Kyn, regulated by IDO1 [40], is known to activate the AhR signaling pathway, crucial for immune regulation [41], and mediate the NF- κ B inflammatory pathway, leading to NLRP3 transcription and inflammasome activation [42]. Immunohistochemistry for AhR in renal tissues revealed increased expression in RETCs following AKI (Fig. 5B). We hypothesized that the increased IFN- γ during AKI enhances the activity of IDO1 in RETCs, thereby activating the AhR/NF- κ B/NLRP3 inflammatory pathway and driving the upregulation of downstream inflammatory cytokines. Western blotting confirmed increased protein expression of IFN- γ , IDO1, AhR, NF- κ B, NLRP3, and IL-1 β in the AKI group.

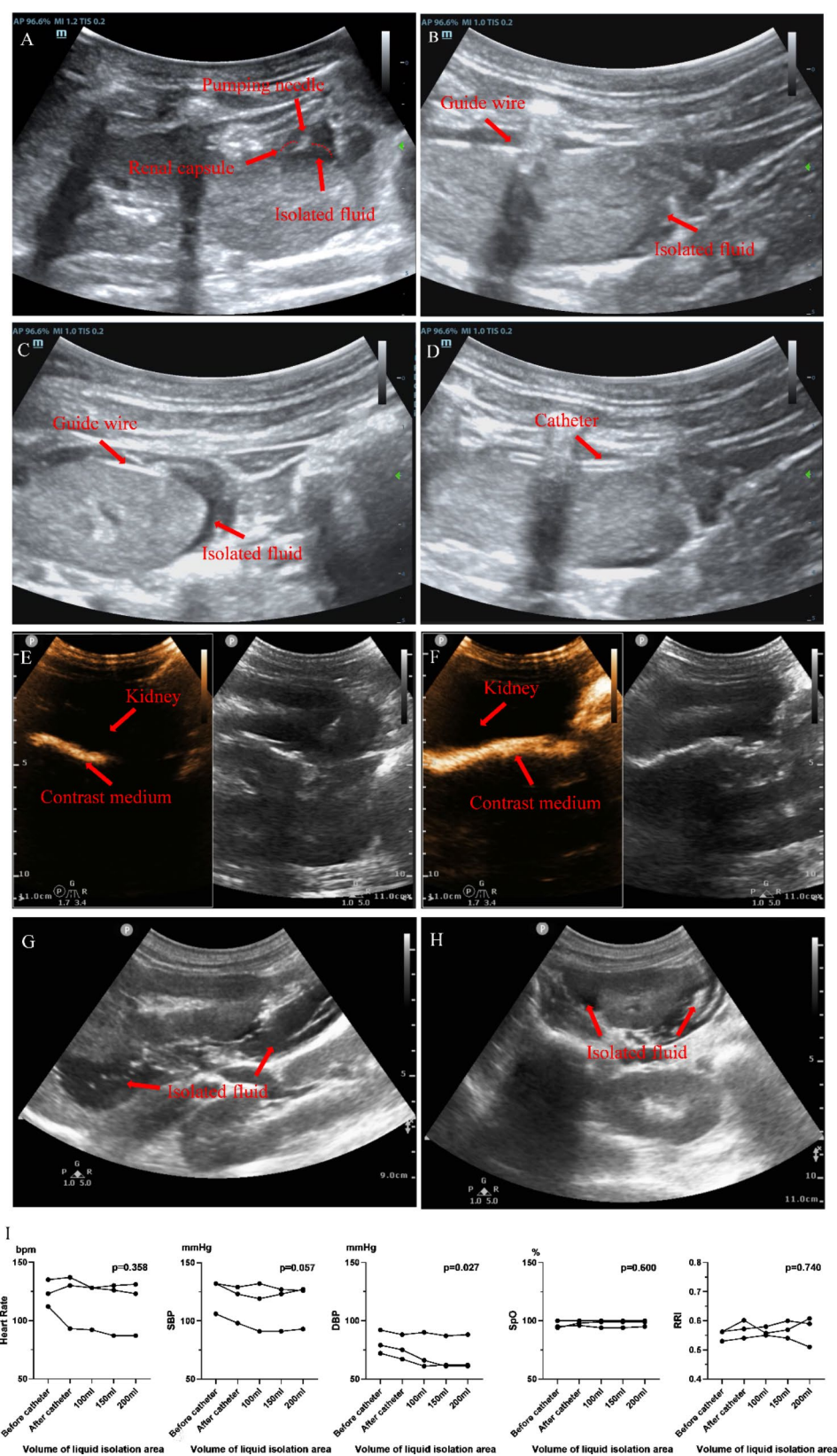


Fig. 3 (See legend on next page.)

(See figure on previous page.)

Fig. 3 Ultrasound-guided renal subcapsular catheterization and safety evaluation **(A)** Blunt separation of renal capsule and parenchyma under ultrasound guidance. **(B)** Guidewire in long-axis view of the kidney. **(C)** Guidewire in short-axis view of the kidney. **(D)** Catheter in long-axis view of the kidney. **(E)** Contrast-enhanced ultrasound imaging after injection of 5 ml contrast agent via renal subcapsular catheter. **(F)** Contrast-enhanced ultrasound imaging after injection of 50 ml contrast agent via renal subcapsular catheter. **(G)** Long-axis view of the kidney after injection of 200 ml of isolated fluid. **(H)** Short-axis view of the kidney after injection of 200 ml of isolated fluid. **(I)** Results of HR, SBP, DBP, SpO₂, and RRI ($n=3$). There is a statistically significant difference at $p<0.05$

Notably, these protein expression levels were significantly reduced in the multiple transplantation group (Fig. 5C).

Tryptophan metabolite kyn mediating AhR/NF- κ B/NLRP3/IL1 β in renal tubular epithelial cells

To substantiate our hypothesis and *in vivo* findings, primary mouse RTECs were stimulated with IFN- γ , leading to increased protein expression of IDO1, AhR, NF- κ B, NLRP3, and IL-1 β , along with elevated Kyn production (Fig. 6A, B and C). Following treatment with Kyn, the 50 ng/ml group showed a significant increase in protein levels of AhR, NF- κ B, NLRP3, and IL-1 β (Fig. 6D). Interestingly, AhR transfected with siRNA abrogated the Kyn-induced upregulation of NF- κ B, NLRP3, and IL-1 β protein expression levels (Fig. 6E). Since the cytokine IL-1 β exhibits synergistic effects with IFN- γ [43, 44], we further stimulated primary RETCs with IL-1 β , IFN- γ , or both combined. Compared to stimulation with either IL-1 β or IFN- γ alone, combined stimulation with both cytokines significantly enhanced IDO1, AhR, NF- κ B, NLRP3, and IL-1 β protein expression (Fig. 6F).

Discussion

To assess the clinical potential of renal subcapsular MSCs transplantation for AKI, we established a minipig AKI model using cisplatin co-administered with hydration. We then evaluated the feasibility and therapeutic efficacy of ultrasound-guided MSC transplantation in this model. Additionally, our findings revealed a significant elevation of the tryptophan metabolite Kyn within RETCs during AKI, that was associated with activation of the AhR-mediated inflammatory pathway, ultimately contributing to kidney injury. Importantly, multiple renal subcapsular transplantation of MSCs demonstrated a superior effect on the recovery of renal function compared to the single transplantation for AKI.

It is now understood that high-dose cisplatin-induced AKI models in minipigs often suffer from severe kidney injury and short animal survival times. These limitations hinder accurate evaluation of intervention efficacy and in-depth studies on potential adverse renal remodeling after AKI. Similar issues plague rodent models of cisplatin-induced AKI [45–47]. In an attempt to address these limitations, researchers have developed chronic fibrosis models using multiple low-dose cisplatin administrations [47–49]. However, these models exhibit significant pathophysiological differences compared to the

high-dose model [50]. Additionally, attempts to establish a rodent AKI model with recovery using multiple medium-dose cisplatin regimens require further optimization to extend animal survival times [51, 52]. To overcome these shortcomings, we propose a minipig AKI model utilizing high-dose cisplatin combined with hydration, which is recognized for its ability to mitigate the severity of kidney injury associated with high-dose cisplatin [30]. This approach offers extended animal survival times exceeding 28 days and facilitates the observation of the entire spectrum of AKI development, recovery, and potential transition to chronic kidney disease (CKD), thereby addressing the limitations of previous cisplatin-induced AKI models.

The rich blood supply beneath the renal capsule [53, 54] makes it a suitable location for transplanting various cell types, including endocrine glands and organoids [55–58]. However, traditional subcapsular transplantation necessitates laparotomy, a more invasive surgical procedure [54, 59]. Additionally, transplanted cells can leak from the subcapsular space, requiring biogels to prevent cell migration [17]. To address these limitations, we propose a minimally invasive approach for subcapsular transplantation using liquid isolation, a technique used in ultrasound-guided radiofrequency ablation therapy that protects surrounding nerves and blood vessels by injecting saline or a glucose solution to create a barrier before thermal ablation [36]. This study is the first to utilize ultrasound-guided renal capsule catheterization to achieve multiple subcapsular MSCs, an approach that successfully overcomes the potential decline in efficacy associated with reduced MSCs activity over time [60–62]. The results related to renal injury and apoptosis suggest that multiple MSCs transplantations yield a more favorable therapeutic effect, mitigate renal damage, and enhance the recovery of renal function, aligning with previous research study [62].

Furthermore, we employed a cumulative cell dose exceeding that used in previous clinical trials, while avoiding the potential embolic risks linked to high cell doses [15, 63]. The catheter outlet placement within the upper third of the kidney ensured MSCs suspension retention within the capsule, eliminating the need for biogels. Moreover, our findings suggest that the short-term presence of isolated fluid during catheterization does not pose a risk of renal compression. The experimental results demonstrate the safety of multiple subcapsular

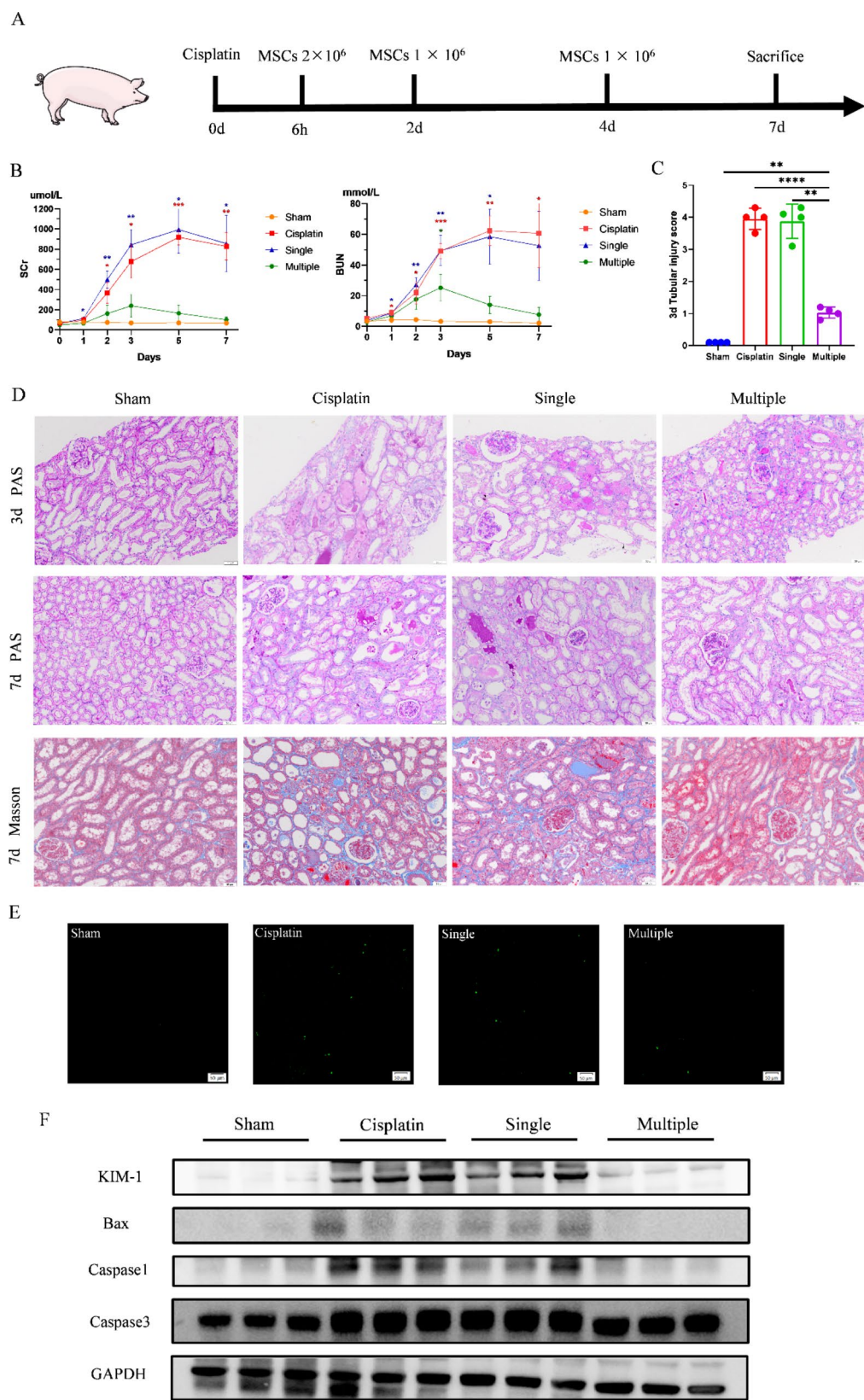


Fig. 4 (See legend on next page.)

(See figure on previous page.)

Fig. 4 Multiple renal subcapsular transplantation of MSCs promoting renal recovery **(A)** Experimental procedures of MSCs therapy for AKI minipigs. **(B)** Serum Scr and BUN of minipigs; statistical analysis results were compared between the cisplatin group, single-transplantation group and multiple-transplantation group and sham, respectively ($n=4$). **(C)** Semi-quantitative analysis of PAS staining at 3d ($n=4$). **(D)** PAS staining at 3d and 7d and Masson staining at 7d (200x). **(E)** and **(F)** TUNEL and KIM-1, Bax, Caspase1, and Caspase3 on immunoblotting at 7d. *, $p<0.05$; **, $p<0.01$; ***, $p<0.001$; ****, $p<0.0001$. Full-length blots are presented in Supplementary Immunoblotting Figs. 19–22

MSCs transplantations under the guidance of ultrasound, warranting further investigation and development for clinical application.

In AKI, RTECs undergo metabolic reprogramming similar to immune cells, and their metabolic processes and metabolites can influence both kidney injury and repair through the innate immune system [64, 65].

Current evidence suggests that tryptophan metabolism plays a pivotal role in this inflammatory response. IFN- γ or TNF- α can induce IDO1, an enzyme that promotes the breakdown of Trp into Kyn, which in turn activates the downstream AhR-mediated inflammatory pathway [40, 66–68], involved in the pathophysiology of numerous illnesses [69–72]. The NF- κ B/NLRP3 pathway is the

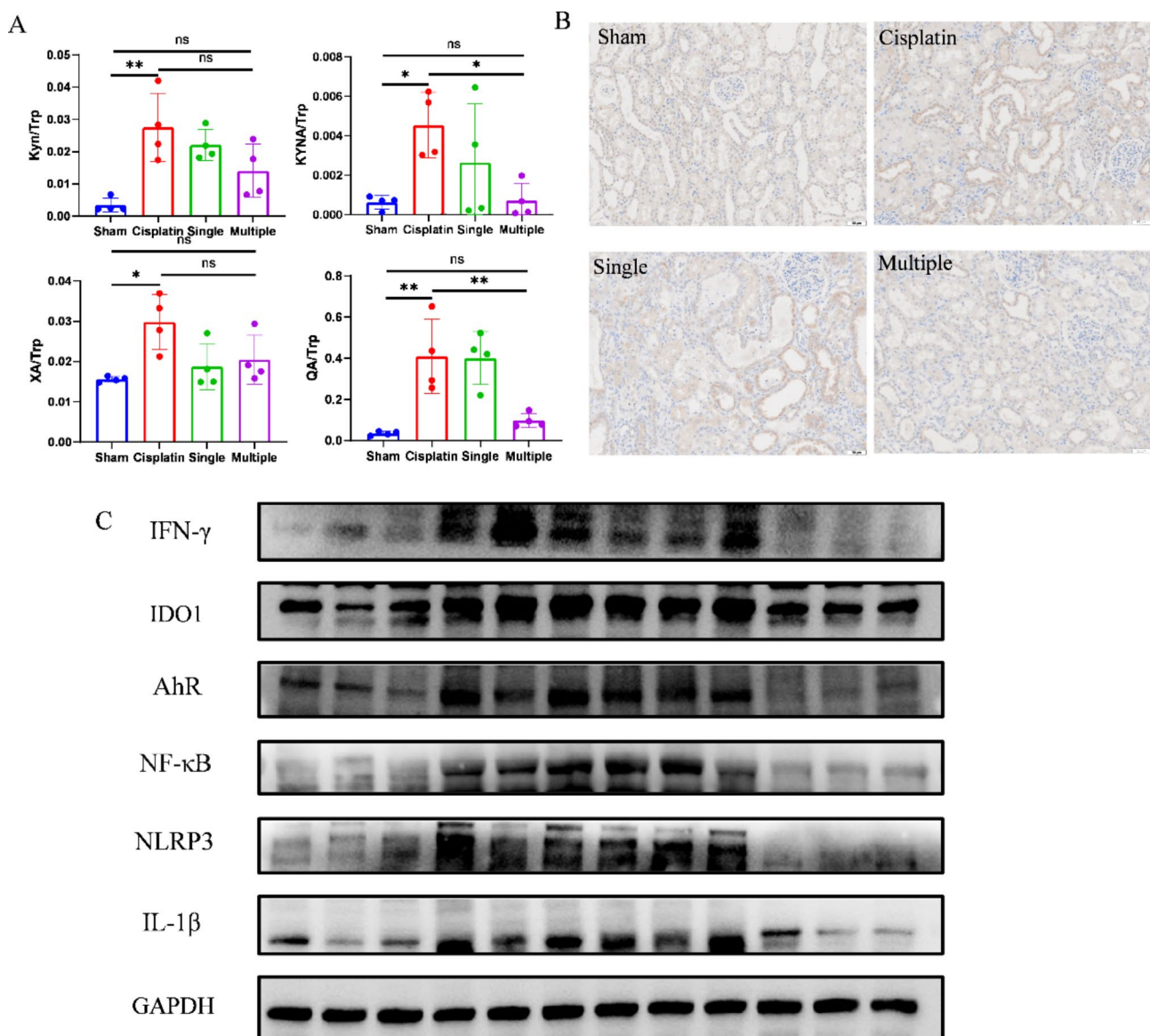


Fig. 5 MSCs alleviate renal tryptophan metabolism disorder and Kyn-mediated AhR/NF- κ B/NLRP3 pathway **(A)** Ratio of kynurenine pathway metabolites Kyn, KYNA, XA, and QA to Trp ($n=4$). **(B)** AhR on IHC at 7d (200x). **(C)** IFN- γ , IDO1, AhR, NF- κ B, NLRP3, and IL-1 β on immunoblotting at 7d. ns, not significant; *, $p<0.05$; **, $p<0.01$. Full-length blots are presented in Supplementary Immunoblotting Figs. 23–28

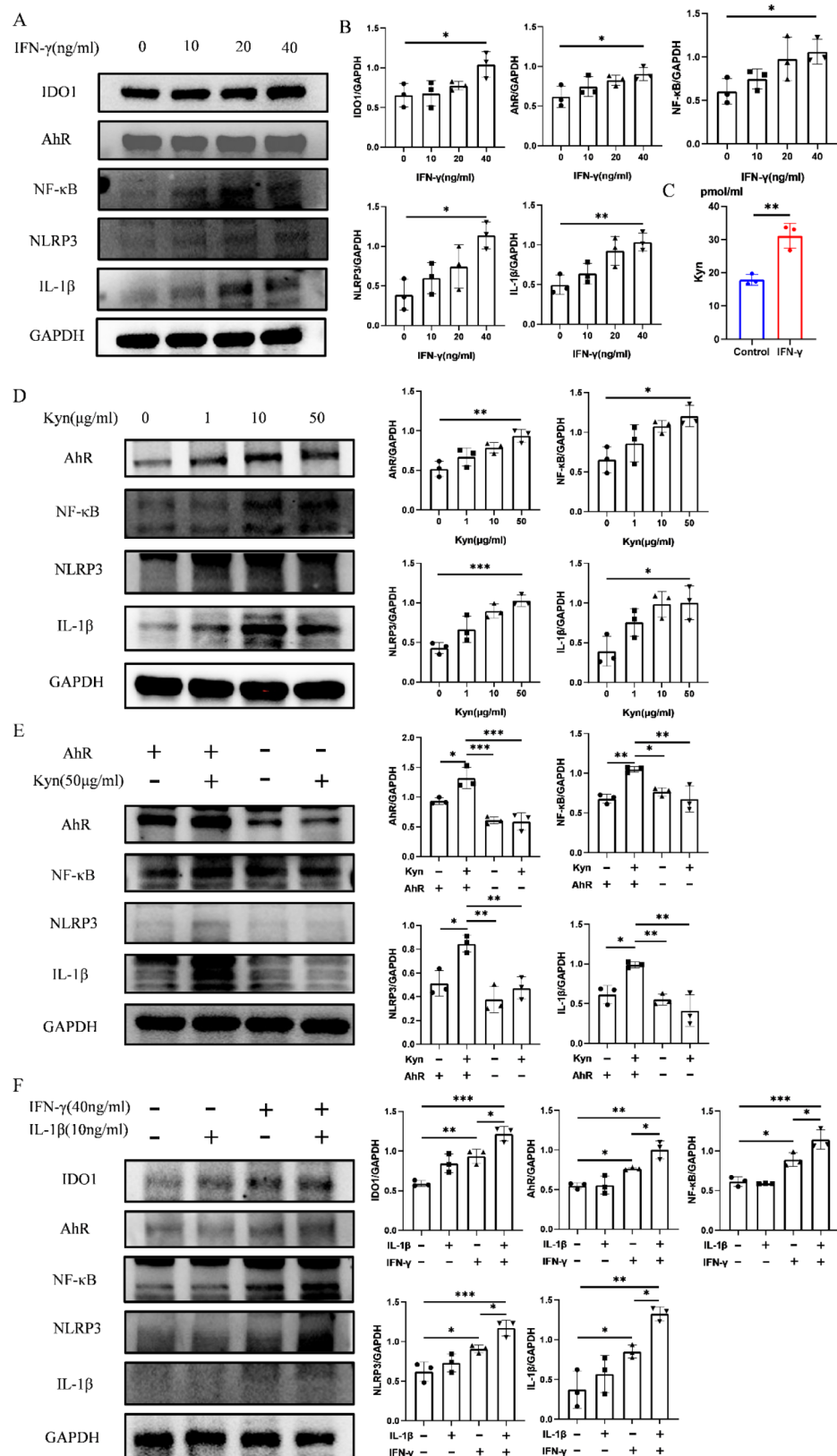


Fig. 6 (See legend on next page.)

(See figure on previous page.)

Fig. 6 Tryptophan metabolite Kyn mediating AhR/NF- κ B/NLRP3/IL1 β in renal tubular epithelial cells **(A)** and **(B)** Protein levels of IDO1, AhR, NF- κ B, NLRP3, and IL-1 β on immunoblotting and semi-quantitative analysis in renal tubular epithelial cells (TREC) after IFN- γ (0, 10, 20, 40ng/ml) stimulation ($n=3$). **(C)** Kyn levels of TREC after IFN- γ (40ng/ml) stimulation ($n=3$). **(D)** Protein levels of AhR, NF- κ B, NLRP3, and IL-1 β on immunoblotting and semi-quantitative analysis in TREC after Kyn (0, 1, 10, 50 μ g/ml) stimulation ($n=3$). **(E)** Protein levels of AhR, NF- κ B, NLRP3, and IL-1 β on immunoblotting and semi-quantitative analysis in TREC with lower expression of AhR after Kyn (50 μ g/ml) stimulation ($n=3$). **(F)** Protein levels of IDO1, AhR, NF- κ B, NLRP3, and IL-1 β on immunoblotting and semi-quantitative analysis in TREC after IL-1 β (10ng/ml) or/and IFN- γ (40ng/ml) stimulation ($n=3$). ns, not significant; *, $p<0.05$; **, $p<0.01$; ***, $p<0.001$; ****, $p<0.0001$. Full-length blots are presented in Supplementary Immunoblotting Figs. 29–82

central innate immune pathway in the kidney [73], initiating the release of a cascade of inflammatory mediators upon activation; notably, AhR can regulate this pathway [74].

Our *in vivo* experiments demonstrated elevated levels of IFN- γ in renal tissue during AKI, coinciding with disruptions in the kynurenine pathway metabolites, a significant increase in Kyn, and enhanced protein expression of the AhR/NF- κ B/NLRP3/IL-1 β inflammatory pathway. *In vitro* studies further corroborated these findings. IFN- γ treatment (40 ng/ml) significantly upregulated IDO1 expression in cells, leading to increased Kyn production and subsequent upregulation of AhR, NF- κ B, NLRP3, and IL-1 β protein levels. These findings suggest that Kyn can exacerbate inflammatory injury in renal tubular cells via the AhR-mediated NF- κ B/NLRP3/IL-1 β pathway. Furthermore, we observed that IL-1 β could work synergistically with IFN- γ to induce IDO1 expression in RETCs. This co-stimulation also upregulated protein levels of AhR, NF- κ B, NLRP3, and IL-1 β , forming a positive feedback loop designated as IL-1 β + IFN- γ - IDO1 - AhR, which collectively amplifies inflammatory injury in RETCs. In conclusion, our study revealed a strong correlation between tryptophan metabolism in RETCs and the innate immune system during AKI.

Our study has several limitations that should be acknowledged. First, due to the large animal model, we lacked suitable *in vivo* techniques to monitor MSCs activity beneath the renal capsule. Second, although the transplantation frequency and dosage were based on clinical trials, future studies should optimize these parameters. Third, while we observed that MSCs alleviate immune metabolic remodeling caused by tryptophan metabolism disorder in kidney, the specific mechanism by which MSCs regulate IFN- γ levels remains unclear. Future studies will investigate whether MSCs modulate IFN- γ levels through interactions with innate immune cells, thereby influencing tryptophan metabolite Kyn and the inflammatory response in RETCs.

Conclusions

In this study, we established a new minipig model of AKI using cisplatin and hydration, allowing for better evaluation of potential therapies. Our minimally invasive approach, ultrasound-guided transplantation of multiple MSCs beneath the renal capsule, demonstrated safety and efficacy in treating AKI, presenting significant

clinical application potential, and introducing an innovative concept for renal subcapsular endocrine gland transplantation or drug administration. Furthermore, we revealed a link between tryptophan metabolism and inflammation in kidney during AKI, suggesting that targeting this pathway could be a future strategy to promote kidney repair.

Abbreviations

AKI	Acute kidney injury
MSCs	Mesenchymal stem cells
Kyn	Kynurenine
AhR	Aryl hydrocarbon receptor
KP	Kynurenine pathway
Trp	Tryptophan
SCr	Serum creatinine
BUN	blood urea nitrogen
IDO1	Indoleamine 2,3-dioxygenase 1
KMO	Kynurenine 3-monooxygenase
KYNU	Kynureninase
HAAO	Hydroxyanthranilic acid 3,4-dioxygenase
QPRT	Quinolinate phosphoribosyltransferase
RRI	Renal resistance index
HR	Heart rate
SBP	Systolic blood pressure
DBP	Diastolic blood pressure
KIM-1	Kidney injury molecule 1
IFN- γ	Interferon gamma
NLRP3	NOD-like receptor thermal protein domain associated protein 3
IL-1 β	Interleukin-1 beta
RETCs	Renal tubular epithelial cells

Supplementary Information

The online version contains supplementary material available at <https://doi.org/10.1186/s13287-025-04137-4>.

Supplementary Material 1

Supplementary Material 2

Acknowledgements

We thank Yunxiao Jia, Bo Peng, and Changqi Zhao from the Laboratory Animal Center of Chinese PLA general hospital for their technical support in the minipig experiments. Additionally, we would like to acknowledge the language editing service provided by the Home for Researchers editorial team (www.home-for-researchers.com). The authors declare that they have not used AI-generated work in this manuscript.

Author contributions

Tuo Xiao, Yuhao Chen, and Bo Jiang contributed equally to this work. Tuo Xiao, Yuhao Chen and Yanjun Liang carried out the minipig experiments. Tuo Xiao and Bo Jiang completed the ultrasound experiments. Tuo Xiao and Mengjie Huang completed the cell experiments. Tuo Xiao and Bo Jiang wrote the manuscript. Wenjuan Wang and Xumin Zheng prepared MSCs suspension and reviewed the manuscript. Guangyan Cai and Xiangmei Chen provided supervision for the study and edited the manuscript. The final manuscript has been read and approved by all authors.

Funding

This study was funded by the National Natural Science Foundation of China (grant no. 82170686) and a grant provided to Guangyan Cai (grant no. 22KJLJ001).

Data availability

All data associated with this study are present in the paper or the Supplement Methods and Materials.

Declarations

Ethical approval

Human umbilical cord blood MSCs used in this study were donated by Wuhan Optic Valley Zhongyuan Pharmaceutical Co. Ltd, which had confirmed that there was initial ethical approval for collection of human cells, and that informed consent was duly signed by the donors. The animal experiments were conducted in line with the ARRIVE guidelines 2.0. All the animal experimental procedures and therapeutic experiment involving MSCs were reviewed and approved by the Institutional Animal Care and Use Committee of the Chinese People's Liberation Army General Hospital. (Project title: Clinical study of stem cell therapy for severe acute kidney injury; Ethics lot number: 2022-X18-22; Date of approval: March 18, 2022).

Consent for publication

Not applicable.

Competing interests

The authors have no conflicting interests.

Author details

¹Department of Nephrology, First Medical Center of Chinese PLA General Hospital, State Key Laboratory of Kidney Diseases, National Clinical Research Center for Kidney Diseases, Beijing Key Laboratory of Kidney Diseases Research, Beijing 100853, China

²Department of Nephrology, The First Affiliated Hospital of Zhengzhou University, Zhengzhou, Henan 450052, China

³Department of Ultrasound, First Medical Centre of Chinese PLA General Hospital, Beijing 100853, China

Received: 8 September 2024 / Accepted: 10 January 2025

Published online: 28 February 2025

References

- Andrade L, Rodrigues CE, Gomes SA, Noronha IL. Acute kidney injury as a Condition of Renal Senescence. *Cell Transpl*. 2018;27(5):739–53.
- Kellum JA, Lameire N. Diagnosis, evaluation, and management of acute kidney injury: a KDIGO summary (part 1). *Crit Care*. 2013;17(1):204.
- Levey AS, James MT. Acute kidney injury. *Ann Intern Med*. 2017;167(9):Itc66–80.
- Susantitaphong P, Cruz DN, Cerda J, Bulfaraj M, Alqahtani F, Koulouridis I, Jaber BL. World incidence of AKI: a meta-analysis. *Clin J Am Soc Nephrol*. 2013;8(9):1482–93.
- Uchino S, Kellum JA, Bellomo R, Doig GS, Morimatsu H, Morgera S, Schetz M, Tan I, Bouman C, Macedo E, et al. Acute renal failure in critically ill patients: a multinational, multicenter study. *JAMA*. 2005;294(7):813–8.
- Li PK, Burdmann EA, Mehta RL. Acute kidney injury: global health alert. *Transplantation*. 2013;95(5):653–7.
- Hoste EA, Schurgers M. Epidemiology of acute kidney injury: how big is the problem? *Crit Care Med*. 2008;36(4 Suppl):S146–151.
- Khawaja A. KDIGO clinical practice guidelines for acute kidney injury. *Nephron Clin Pract*. 2012;120(4):c179–184.
- Moore PK, Hsu RK, Liu KD. Management of Acute kidney Injury: Core Curriculum 2018. *Am J Kidney Dis*. 2018;72(1):136–48.
- Ostermann M, Liu K, Kashani K. Fluid Management in Acute kidney Injury. *Chest*. 2019;156(3):594–603.
- Han Q, Wang X, Ding X, He J, Cai G, Zhu H. Immunomodulatory effects of mesenchymal stem cells on Drug-Induced Acute kidney Injury. *Front Immunol*. 2021;12:683003.
- Morigi M, Imberti B, Zoja C, Corna D, Tomasoni S, Abbate M, Rottoli D, Angioletti S, Benigni A, Perico N, et al. Mesenchymal stem cells are renotropic, helping to repair the kidney and improve function in acute renal failure. *J Am Soc Nephrol*. 2004;15(7):1794–804.
- Selim RE, Ahmed HH, Abd-Allah SH, Sabry GM, Hassan RE, Khalil WKB, Abouhashem NS. Mesenchymal stem cells: a Promising Therapeutic Tool for Acute kidney Injury. *Appl Biochem Biotechnol*. 2019;189(1):284–304.
- Cheng K, Rai P, Plagov A, Lan X, Kumar D, Salhan D, Rehman S, Malhotra A, Bhargava K, Palestro CJ, et al. Transplantation of bone marrow-derived MSCs improves cisplatin-induced renal injury through paracrine mechanisms. *Exp Mol Pathol*. 2013;94(3):466–73.
- Swaminathan M, Stafford-Smith M, Chertow GM, Warnock DG, Paragamian V, Brenner RM, Lellouche F, Fox-Robichaud A, Atta MG, Melby S, et al. Allogeneic mesenchymal stem cells for treatment of AKI after Cardiac surgery. *J Am Soc Nephrol*. 2018;29(1):260–7.
- Eggenhofer E, Benseler V, Kroemer A, Popp FC, Geissler EK, Schlitt HJ, Baan CC, Dahlke MH, Hoogduijn MJ. Mesenchymal stem cells are short-lived and do not migrate beyond the lungs after intravenous infusion. *Front Immunol*. 2012;3:297.
- Wang W, Zhang M, Ren X, Song Y, Xu Y, Zhuang K, Xiao T, Guo X, Wang S, Hong Q, et al. Single-cell dissection of cellular and molecular features underlying mesenchymal stem cell therapy in ischemic acute kidney injury. *Mol Ther*. 2023;31(10):3067–83.
- Han Q, Ai S, Hong Q, Zhang C, Song Y, Wang X, Wang X, Cui S, Li Z, Zhu H, et al. A supramolecular hydrogel based on the combination of YIGSR and RGD enhances mesenchymal stem cells paracrine function via integrin $\alpha 2 \beta 1$ and PI3K/AKT signaling pathway for acute kidney injury therapy. *Chem Eng J*. 2022;436:135088.
- Wu D, Zou S, Chen H, Li X, Xu Y, Zuo Q, Pan Y, Jiang SW, Huang H, Sun L. Transplantation routes affect the efficacy of human umbilical cord mesenchymal stem cells in a rat GDM model. *Clin Chim Acta*. 2017;475:137–46.
- Cervenka I, Agudelo LZ, Ruas JL. Kynurenines: Tryptophan's metabolites in exercise, inflammation, and mental health. *Science*. 2017; 357(6349).
- Castro-Portuguez R, Sutphin GL. Kynurenine pathway, NAD(+) synthesis, and mitochondrial function: targeting tryptophan metabolism to promote longevity and healthspan. *Exp Gerontol*. 2020;132:110841.
- Huang T, Song J, Gao J, Cheng J, Xie H, Zhang L, Wang YH, Gao Z, Wang Y, Wang X, et al. Adipocyte-derived kynurenine promotes obesity and insulin resistance by activating the AhR/STAT3/IL-6 signaling. *Nat Commun*. 2022;13(1):3489.
- Ren R, Fang Y, Sherchan P, Lu Q, Lenahan C, Zhang JH, Zhang J, Tang J. Kynurenine/Aryl hydrocarbon receptor modulates mitochondria-mediated oxidative stress and neuronal apoptosis in experimental intracerebral hemorrhage. *Antioxid Redox Signal*. 2022;37(16–18):1111–29.
- Zhang Q, Sun Y, He Z, Xu Y, Li X, Ding J, Lu M, Hu G. Kynurenine regulates NLRP2 inflammasome in astrocytes and its implications in depression. *Brain Behav Immun*. 2020;88:471–81.
- Brandacher G, Cakar F, Winkler C, Schneeberger S, Obrist P, Bösmüller C, Werner-Felmayer G, Werner ER, Bonatti H, Margreiter R, et al. Non-invasive monitoring of kidney allograft rejection through IDO metabolism evaluation. *Kidney Int*. 2007;71(1):60–7.
- Zhang F, Wang Q, Xia T, Fu S, Tao X, Wen Y, Chan S, Gao S, Xiong X, Chen W. Diagnostic value of plasma tryptophan and symmetric dimethylarginine levels for acute kidney injury among tacrolimus-treated kidney transplant patients by targeted metabolomics analysis. *Sci Rep*. 2018;8(1):14688.
- Tan B, Chen J, Qin S, Liao C, Zhang Y, Wang D, Li S, Zhang Z, Zhang P, Xu F. Tryptophan pathway-targeted Metabolomics Study on the mechanism and intervention of Cisplatin-Induced Acute kidney Injury in rats. *Chem Res Toxicol*. 2021;34(7):1759–68.
- Wang SY, Zhang CY, Cai GY, Chen XM. Method used to establish a large animal model of drug-induced acute kidney injury. *Exp Biol Med (Maywood)*. 2021;246(8):986–95.
- Chen JW, Huang MJ, Chen XN, Wu LL, Li QG, Hong Q, Wu J, Li F, Chen LM, Dong Y, et al. Transient upregulation of EGR1 signaling enhances kidney repair by activating SOX9(+) renal tubular cells. *Theranostics*. 2022;12(12):5434–50.
- Cornellison TL, Reed E. Nephrotoxicity and hydration management for cisplatin, carboplatin, and ormaplatin. *Gynecol Oncol*. 1993;50(2):147–58.
- Ronco C, Bellomo R, Kellum JA. Acute kidney injury. *Lancet*. 2019;394(10212):1949–64.
- Krupa A, Krupa MM, Pawlak K. Indoleamine 2,3 dioxygenase 1-The potential link between the Innate immunity and the Ischemia-Reperfusion-Induced Acute kidney Injury? *Int J Mol Sci* 2022, 23(11).

33. Zheng X, Zhang A, Binnie M, McGuire K, Webster SP, Hughes J, Howie SEM, Mole DJ. Kynurenine 3-monooxygenase is a critical regulator of renal ischemia-reperfusion injury. *Exp Mol Med*. 2019;51(2):1–14.
34. Späth MR, Hoyer-Allo KJR, Seufert L, Höhne M, Lucas C, Bock T, Isermann L, Brodesser S, Lackmann JW, Kiefer K, et al. Organ Protection by Caloric Restriction depends on activation of the De Novo NAD⁺ synthesis pathway. *J Am Soc Nephrol*. 2023;34(5):772–92.
35. Clark AJ, Saade MC, Vemireddy V, Vu KQ, Flores BM, Etzrodt V, Ciampa EJ, Huang H, Takakura A, Zandi-Nejad K, et al. Hepatocyte nuclear factor 4a mediated quinolinate phosphoribosyltransferase (QPRT) expression in the kidney facilitates resilience against acute kidney injury. *Kidney Int*. 2023;104(6):1150–63.
36. Liu F, Liu Y, Peng C, Yu M, Wu S, Qian L, Han Z, Yu J, Chai H, Liang P. Ultrasound-guided microwave and radiofrequency ablation for primary hyperparathyroidism: a prospective, multicenter study. *Eur Radiol*. 2022;32(11):7743–54.
37. Yilmaz S, Zor M, Ersan M, Hamcan S. Bilateral massive perirenal subcapsular effusion: a case report. *J Clin Ultrasound*. 2017;45(9):597–9.
38. Haydar A, Bakri RS, Prime M, Goldsmith DJ. Page kidney—a review of the literature. *J Nephrol*. 2003;16(3):329–33.
39. De Hert S, Moerman A, Sevoflurane. F1000Res 2015, 4(F1000 Faculty Rev):626.
40. Lashgari NA, Roudsari NM, Shayan M, Niazi Shahrafi F, Hosseini Y, Momtaz S, Abdolghaffari AH. IDO/Kynurenine; novel insight for treatment of inflammatory diseases. *Cytokine*. 2023;166:156206.
41. Opitz CA, Litzenburger UM, Sahm F, Ott M, Tritschler I, Trump S, Schumacher T, Jestaedt L, Schrenk D, Weller M, et al. An endogenous tumour-promoting ligand of the human aryl hydrocarbon receptor. *Nature*. 2011;478(7368):197–203.
42. Yamaguchi K, Yisireyli M, Goto S, Cheng XW, Nakayama T, Matsushita T, Niwa T, Murohara T, Takeshita K. Indoxyl sulfate activates NLRP3 inflammasome to Induce Cardiac Contractile Dysfunction accompanied by myocardial fibrosis and hypertrophy. *Cardiovasc Toxicol*. 2022;22(4):365–77.
43. Sheng H, Wang Y, Jin Y, Zhang Q, Zhang Y, Wang L, Shen B, Yin S, Liu W, Cui L, et al. A critical role of IFN γ in priming MSC-mediated suppression of T cell proliferation through up-regulation of B7-H1. *Cell Res*. 2008;18(8):846–57.
44. Jiang K, Zhang Y, He F, Zhang M, Li T, Tu Z, Xu D, Zhang M, Han L, Guo L, et al. A negative feedback loop involving NF- κ B/TIR8 regulates IL-1 β -induced epithelial-myofibroblast transdifferentiation in human tubular cells. *J Cell Commun Signal*. 2021;15(3):393–403.
45. Huang J, Bayliss G, Zhuang S. Porcine models of acute kidney injury. *Am J Physiol Ren Physiol*. 2021;320(6):F1030–44.
46. Ferenbach DA, Bonventre JV. Mechanisms of maladaptive repair after AKI leading to accelerated kidney ageing and CKD. *Nat Rev Nephrol*. 2015;11(5):264–76.
47. Sharp CN, Siskind LJ. Developing better mouse models to study cisplatin-induced kidney injury. *Am J Physiol Ren Physiol*. 2017;313(4):F835–41.
48. Landau SJ, Guo X, Velazquez H, Torres R, Olson E, Garcia-Milian R, Moeckel GW, Desir GV, Safirstein R. Regulated necrosis and failed repair in cisplatin-induced chronic kidney disease. *Kidney Int*. 2019;95(4):797–814.
49. Lee YJ, Li KY, Wang PJ, Huang HW, Chen MJ. Alleviating chronic kidney disease progression through modulating the critical genus of gut microbiota in a cisplatin-induced Lanyu pig model. *J Food Drug Anal*. 2020;28(1):103–14.
50. Sears SM, Siskind LJ. Potential therapeutic targets for Cisplatin-Induced kidney Injury: lessons from other models of AKI and Fibrosis. *J Am Soc Nephrol*. 2021;32(7):1559–67.
51. Torres R, Velazquez H, Chang JJ, Levene MJ, Moeckel G, Desir GV, Safirstein R. Three-dimensional morphology by Multiphoton Microscopy with Clearing in a Model of Cisplatin-Induced CKD. *J Am Soc Nephrol*. 2016;27(4):1102–12.
52. Katagiri D, Hamasaki Y, Doi K, Negishi K, Sugaya T, Nangaku M, Noiri E. Interstitial renal fibrosis due to multiple cisplatin treatments is ameliorated by semicarbazide-sensitive amine oxidase inhibition. *Kidney Int*. 2016;89(2):374–85.
53. van den Berg CW, Ritsma L, Avramut MC, Wiersma LE, van den Berg BM, Leuning DG, Lievers E, Koning M, Vanslambrouck JM, Koster AJ, et al. Renal subcapsular transplantation of PSC-Derived kidney Organoids induces neo-vasculogenesis and significant glomerular and tubular maturation in vivo. *Stem Cell Rep*. 2018;10(3):751–65.
54. Smood B, Bottino R, Hara H, Cooper DKC. Is the renal subcapsular space the preferred site for clinical porcine islet xenotransplantation? Review article. *Int J Surg*. 2019;69:100–7.
55. Lorenzini L, Campodonico A, Tota G. [Survival of homotransplanted adrenal cortex tissue in the subcapsular space of the kidney]. *Studi Sassar*. 1965;43(3):193–206.
56. Wang F, Tian Y, Huang L, Qin T, Ma W, Pei C, Xu B, Han H, Liu X, Pan P, et al. Roles of follicle stimulating hormone and sphingosine 1-phosphate co-administered in the process in mouse ovarian vitrification and transplantation. *J Ovarian Res*. 2023;16(1):173.
57. Dai X, Zhao J, Hua L, Chen H, Liang C. Thymus transplantation regulates blood pressure and alleviates hypertension-associated heart and kidney damage via transcription factors FoxN1 pathway. *Int Immunopharmacol*. 2023;116:109798.
58. Xinaris C, Benedetti V, Rizzo P, Abbate M, Corna D, Azzollini N, Conti S, Unbekandt M, Davies JA, Morigi M, et al. In vivo maturation of functional renal organoids formed from embryonic cell suspensions. *J Am Soc Nephrol*. 2012;23(11):1857–68.
59. Shultz LD, Goodwin N, Ishikawa F, Hosur V, Lyons BL, Greiner DL. Subcapsular transplantation of tissue in the kidney. *Cold Spring Harb Protoc*. 2014;2014(7):737–40.
60. Huang M, Li D, Chen J, Ji Y, Su T, Chen Y, Zhang Y, Wang Y, Li F, Chen S, et al. Comparison of the treatment efficacy of umbilical mesenchymal stem cell transplantation via renal subcapsular and parenchymal routes in AKI-CKD mice. *Stem Cell Res Ther*. 2022;13(1):128.
61. Ho JH, Tseng TC, Ma WH, Ong WK, Chen YF, Chen MH, Lin MW, Hong CY, Lee OK. Multiple intravenous transplantations of mesenchymal stem cells effectively restore long-term blood glucose homeostasis by hepatic engraftment and β -cell differentiation in streptozocin-induced diabetic mice. *Cell Transpl*. 2012;21(5):997–1009.
62. Lv X, Guan C, Li Y, Su X, Zhang L, Wang X, Xia HF, Ma X. Effects of single and multiple transplantations of human umbilical cord mesenchymal stem cells on the recovery of ovarian function in the treatment of premature ovarian failure in mice. *J Ovarian Res*. 2021;14(1):119.
63. Li X, Huang Q, Zhang X, Xie C, Liu M, Yuan Y, Feng J, Xing H, Ru L, Yuan Z, et al. Reproductive and Developmental Toxicity Assessment of Human umbilical cord mesenchymal stem cells in rats. *Front Cell Dev Biol*. 2022;10:883996.
64. Xu Y, Ma H, Shao J, Wu J, Zhou L, Zhang Z, Wang Y, Huang Z, Ren J, Liu S, et al. A role for tubular necrosis in Cisplatin-Induced AKI. *J Am Soc Nephrol*. 2015;26(11):2647–58.
65. van der Rijt S, Leemans JC, Florquin S, Houtkooper RH, Tammaro A. Immunometabolic rewiring of tubular epithelial cells in kidney disease. *Nat Rev Nephrol*. 2022;18(9):588–603.
66. Arnhard K, Pitterl F, Sperner-Unterwieser B, Fuchs D, Koal T, Oberacher H. A validated liquid chromatography-high resolution-tandem mass spectrometry method for the simultaneous quantitation of tryptophan, kynurenine, kynurenic acid, and quinolinic acid in human plasma. *Electrophoresis*. 2018;39(9–10):1171–80.
67. Michaudel C, Danne C, Agus A, Magniez A, Aucouturier A, Spatz M, Lefevre A, Kirchgessner J, Rolhion N, Wang Y, et al. Rewiring the altered tryptophan metabolism as a novel therapeutic strategy in inflammatory bowel diseases. *Gut*. 2023;72(7):1296–307.
68. Pacheco JHL, Elizondo G. Interplay between Estrogen, Kynurenine, and AHR pathways: an immunosuppressive axis with therapeutic potential for breast cancer treatment. *Biochem Pharmacol*. 2023;217:115804.
69. Bhatt S, Devadoss T, Jha NK, Baidya M, Gupta G, Chellappan DK, Singh SK, Dua K. Targeting inflammation: a potential approach for the treatment of depression. *Metab Brain Dis*. 2023;38(1):45–59.
70. Huang YS, Ogbechi J, Clancy FI, Williams RO, Stone TW. IDO and Kynurenine metabolites in Peripheral and CNS disorders. *Front Immunol*. 2020;11:388.
71. Cheong JE, Sun L. Targeting the IDO1/TDO2-KYN-AhR pathway for Cancer Immunotherapy - challenges and opportunities. *Trends Pharmacol Sci*. 2018;39(3):307–25.
72. Xue C, Li G, Zheng Q, Gu X, Shi Q, Su Y, Chu Q, Yuan X, Bao Z, Lu J, et al. Tryptophan metabolism in health and disease. *Cell Metab*. 2023;35(8):1304–26.
73. Andrade-Oliveira V, Foresto-Neto O, Watanabe IKM, Zatz R, Câmara NOS. Inflammation in renal diseases: New and Old players. *Front Pharmacol*. 2019;10:1192.
74. Li L, He G, Shi M, Zhu J, Cheng Y, Chen Y, Chen J, Xue Q. Edaravone dextran ameliorates cognitive impairment by regulating the NF- κ B pathway through AHR and promoting microglial polarization towards the M2 phenotype in mice with bilateral carotid artery stenosis (BCAS). *Eur J Pharmacol*. 2023;957:176036.

Publisher's note

Springer Nature remains neutral with regard to jurisdictional claims in published maps and institutional affiliations.